Materials Research Proceedings 28 (2023) 1481-1490 https://doi.org/10.21741/9781644902479-160

Considering the stiffness of the forming tools in the numerical analysis of the ironing process

OLIVEIRA Marta C.[1,a *], NETO Diogo M.[1,b], ALVES José L.[2,c] and MENEZES Luís F.[1,d]

[1]CEMMPRE, Department of Mechanical Engineering, University of Coimbra, Pinhal de Marrocos, 3030-788 Coimbra, Portugal

[2]Microelectromechanical Systems Research Unit, University of Minho, Campus de Azurém, Guimarães, 4800-058, Portugal

[a]marta.oliveira@dem.uc.pt, [b]diogo.neto@dem.uc.pt, [c]jlalves@dem.uminho.pt, [d]luis.menezes@dem.uc.pt

Keywords: Sheet Metal Forming, Ironing Stage, Deformable Tools, Numerical Analysis

Abstract. Ironing can occur in cylindrical cup drawing whenever the thickness of the drawn flange is larger than the gap between the punch and the die. This is particularly relevant for materials that present *r*-values lower than 1.0, such as the aluminium alloys, since they tend to present more thickening of the flange. The aim of this study is to evaluate numerically the impact of the elastic deformation of the forming tools on the final cup geometry, i.e., the earing profile and the evolution of thickness along the circumferential direction, at different heights. Different contact conditions are also analysed since they strongly affect both the thickness strain and the earing profile. The process conditions considered are the ones from EXACT, the ESAFORM Benchmark 2021, enabling the comparison with experimental results. Considering the deformation of the forming tools mainly impacts the ironing stage, enabling predicting wall thickness values larger than the gap between the punch and the die.

Introduction

Ironing processes are commonly adopted in deep drawing to produce cylindrical cups with uniform thickness in the wall. It is mainly a bulk forming process where the wall of the cup is submitted to compression in the radial direction and shear stress in the contact areas with the tools. These compression forces can result in the elastic deformation of the forming tools, changing the desired thickness reduction. Typically, finite element analysis of sheet metal forming processes assume that the forming tools are rigid. This allows a significant reduction of the computational cost of the simulations since only the outer surface of the tools is modelled. Indeed, in most cases this simplification generates accurate results.

The actual increasing accuracy of both the plasticity and the friction models in predicting the material flow raised questions regarding the influence of the elastic deformations of dies and press lines. In fact, nowadays, it is consensual that they are responsible for many of the differences between the forming simulation results and the manufactured geometries. The iterative spotting steps performed during the die try-out aim to homogenize the contact pressure within the die, to compensate for the fact that the elastic deformation is unknown [1]. Different methods for analysis and virtual rework of tool structures and surfaces, including the combination of structural behaviour with sheet metal forming simulations are described in [2]. The results show that the elastic deformation of the tools changes the blank draw-in significantly, leading to considerable changes in the product's quality measures [2]. Nevertheless, many of the methods suggested to combine the structural analysis and forming simulation into one FE-model lead to large models, which are time-consuming to solve when scaled to industrial dies. Therefore, work has been done

Content from this work may be used under the terms of the Creative Commons Attribution 3.0 license. Any further distribution of this work must maintain attribution to the author(s) and the title of the work, journal citation and DOI. Published under license by Materials Research Forum LLC.

to develop methods to include die and press deformations in sheet metal forming simulations, where the die surfaces are still represented as 2D surfaces [3], including some to circumvent the fact that the press stiffness is commonly unknown [4]. The models that enable predicting the elastic deformations of dies can also be used to improve their structure using, for example, topology optimization [1]. Nevertheless, reliable results require accurate plasticity and the friction models, as pointed out in [2,3].

For small industrial or experimental dies, it is possible to combine structural analysis with sheet metal forming simulations, without resorting to model reduction strategies. This allows an improved understanding of the evolution of the contact conditions during the forming process and its impact in the final geometry. This can be particularly relevant for processes that involve high contact forces, such as the ones that occur in the ironing process. The Swift cup drawing test proposed under the benchmark EXACT [5] was adopted in the present study to assess the importance of the stiffness of the forming tools on the numerical predictions, in particular their accurate dimensions. Accordingly, the finite element model considers that the forming tools are modelled either as rigid or as deformable bodies [6]. Then, the numerical results are compared with the experimental ones, highlighting the impact of the tools deformation in the ironing stage.

Finite Element Model

The benchmark EXACT - Experiment and Analysis of Aluminium Cup Drawing Test [5], proposed at ESAFORM 2021, was selected to analyse the effect of the forming tools stiffness on the ironing conditions. The forming process involves a punch, a die and a blank-holder. Nevertheless, due to the thickening of the flange, the drawing operation is followed by an ironing one, promoted by the same forming tools. The blank presents a diameter 107.5 mm and a nominal thickness of 1.0 mm. The cylindrical punch presents 60 mm of diameter while the die opening diameter is 62.4 mm, i.e., the gap between the punch and the die is 1.2 mm. The cylindrical cup is fully drawn considering a constant blank-holder force of 40 kN. To avoid the pinching of the cup rim by the blank-holder, a stopper with the same thickness of the blank was used, guaranteeing a minimum gap between the blank-holder and the die (1.0 mm) [5].

The numerical simulations are performed with the in-house finite element code DD3IMP [7]. Due to geometrical and material symmetry, only a quarter of the geometry was modelled. The blank was discretized with linear hexahedral finite elements, combined with a selective reduced integration technique. Note that the use of solid elements seems to be the more accurate approach to predict the forming forces and strains (see also [5,8]). Two layers of elements were adopted through the thickness, which allows an accurate evaluation of the contact forces and of the through thickness stress gradients. The region corresponding to the bottom of the cup was defined with an unstructured coarse mesh while for the zone corresponding to the cup wall a refined structured mesh was used, yielding a total of 15,408 finite elements and 16,006 nodes.

Typically, the forming tools are modelled as rigid surfaces. Accordingly, Fig. 1 (a) presents the forming tools modelled by Nagata patches [9], which allows the use of a coarse finite element mesh to define the outer surface of the tools. In addition to the classical approach (rigid tools), the forming tools were also modelled as deformable elastic bodies (E=210 GPa and ν=0.3). The prediction of the elastic deformation of the forming tools requires a proper definition of the geometry (volume) of each one, particularly the punch and the die used in the ironing operation. Two different geometries for the die were studied and modelled by solid elements, which are illustrated in Fig. 1 (b) and (c). The main differences are in the outer diameter and height. The model (#1) presented in Fig. 1 (b) presents an outer diameter of 230 mm and 63 mm of height, while the model (#2) presented in Fig. 1 (c) contains an outer diameter of 180 mm and 25 mm of height. Considering the deformable tools, the total number of elements involved in the numerical simulation increased up to 24,704 elements in model #1 and 23,580 elements in model #2. To impose a constant force over the deformable blank-holder, a pliable (E=0.70 GPa) hollow cylinder

(61 mm of inner diameter and 100 mm of outer diameter) was used with a prescribed displacement on the upper face (1.07 mm). The friction conditions between the blank and the forming tools were described with the Coulomb's law. Two different values of the friction coefficient were adopted in the numerical study to best describe the drawing and the ironing force, respectively.

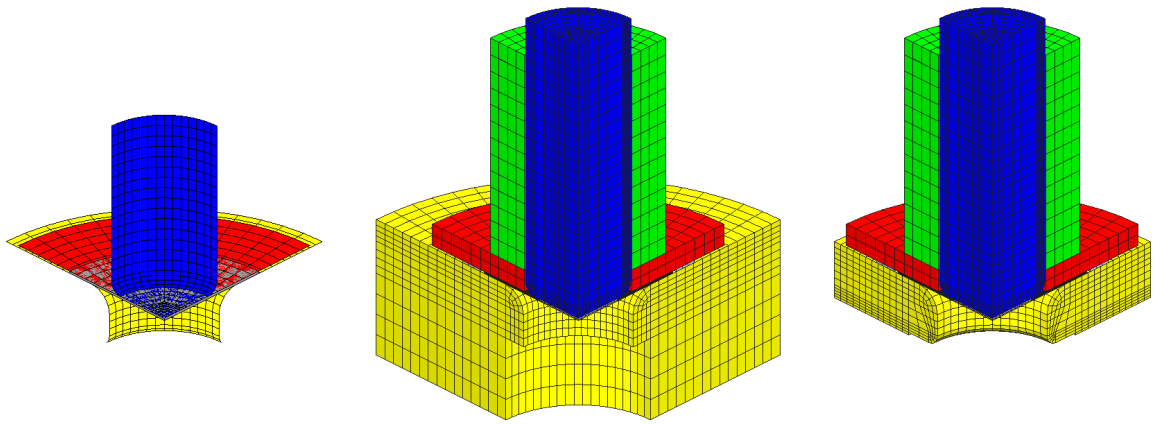

(a) (b) (c)

Fig. 1. Definition of the forming tools used in the numerical simulation: (a) rigid tools described by Nagata patches; (b) deformable tools (#1) described by solid elements; (c) deformable tools (#2) described by solid elements.

Constitutive Model

The mechanical behaviour of the AA 6016-T4 aluminium alloy is assumed to be isotropic in the elastic regime, being described by the Young's modulus, E, and the Poisson ratio, ν. Regarding the hardening behaviour, it was described with the Swift law:

$$Y = K(\varepsilon_0 + \bar{\varepsilon}^{\mathrm{p}})^n \tag{1}$$

where Y is the flow stress, $\bar{\varepsilon}^{\mathrm{p}}$ is the equivalent plastic strain and K, ε_0 and n are material parameters. The values considered for these parameters are the ones suggested by the benchmark committee, as shown in Table 1 [5]. The orthotropic behaviour was described by the yield criterion proposed by Cazacu and Barlat, usually referred as CB2001 [10]. The CB2001 is a generalization of the Drucker's isotropic criterion to orthotropy, such that:

$$\bar{\sigma} = \left\{27\left[\left(J_2^0\right)^3 - c\left(J_3^0\right)^2\right]\right\}^{\frac{1}{6}} \tag{2}$$

where J_2^0 and J_3^0 are the second and third generalized invariants of the deviatoric Cauchy stress tensor, defined as:

$$J_2^0 = \frac{a_1}{6}(\sigma_{11} - \sigma_{22})^2 + \frac{a_2}{6}(\sigma_{11} - \sigma_{33})^2 + \frac{a_3}{6}(\sigma_{11} - \sigma_{33})^2 + a_4\sigma_{12}^2 + a_5\sigma_{13}^2 + a_6\sigma_{23}^2 \tag{3}$$

$$
\begin{aligned}
J_3^0 = {} & (1/27)(b_1+b_2)\sigma_{11}^3 + (1/27)(b_3+b_4)\sigma_{22}^3 + (1/27)[2(b_1+b_4)-b_2-b_3]\sigma_{33}^3 \\
& -(1/9)(b_1\sigma_{22}+b_2\sigma_{33})\sigma_{11}^2 - (1/9)(b_3\sigma_{33}+b_4\sigma_{11})\sigma_{22}^2 \\
& -(1/9)[(b_1-b_2+b_4)\sigma_{11}+(b_1-b_3+b_4)\sigma_{22}]\sigma_{33}^2 \\
& +(2/9)(b_1+b_4)\sigma_{11}\sigma_{22}\sigma_{33} - (\sigma_{13}^2/3)[2b_9\sigma_{22}-b_8\sigma_{33}-(2b_9-b_8)\sigma_{11}] \\
& -(\sigma_{12}^2/3)[2b_{10}\sigma_{33}-b_5\sigma_{22}-(2b_{10}-b_5)\sigma_{11}] - (\sigma_{23}^2/3)[(b_6-b_7)\sigma_{11}-b_6\sigma_{22}-b_7\sigma_{33}] \\
& +2b_{11}\sigma_{12}\sigma_{23}\sigma_{13}
\end{aligned} \tag{4}
$$

where $a_1,...,a_6$ and $b_1,...,b_{11}$ are the anisotropy parameters and c is a weighting parameter. The procedure adopted for the identification of the anisotropy parameters is detailed in [5] and the corresponding values are listed in Table 2. Note that the a_5, a_6 and b_k $(k = 6, 7, 8, 9, 11)$ are the anisotropy parameters corresponding to the off-plane properties, for which the isotropic values, i.e., 1.0 are assumed. Fig. 2 compares the uniaxial tensile tests experimental results (obtained by the Tokyo University of Agriculture and Technology (TUAT) and by the University of Aveiro (UA)) with the ones predicted by CB2001 yield criterion. Note that the in-plane evolution of the *r*-values is well captured but the same is not valid for the yield stress distribution. Although not shown here, the direction of the plastic strain-rate is also well captured by this yield criterion (see [5]).

Table 1. Elastic properties and hardening parameters used in the Swift law [5].

E [GPa]	ν [-]	K [MPa]	ε_0 [-]	n [-]
70	0.33	498.8	0.0089	0.285

Table 2. Anisotropy parameters of CB2001 yield criterion [5].

a_1	a_2	a_3	a_4	a_5	a_6	c				
1.000	1.900	1.391	0.870	1.000	1.000	1.2				
b_1	b_2	b_3	b_4	b_5	b_6	b_7	b_8	b_9	b_{10}	b_{11}
2.000	0.830	1.500	2.000	0.200	1.000	1.000	1.000	1.000	0.566	1.000

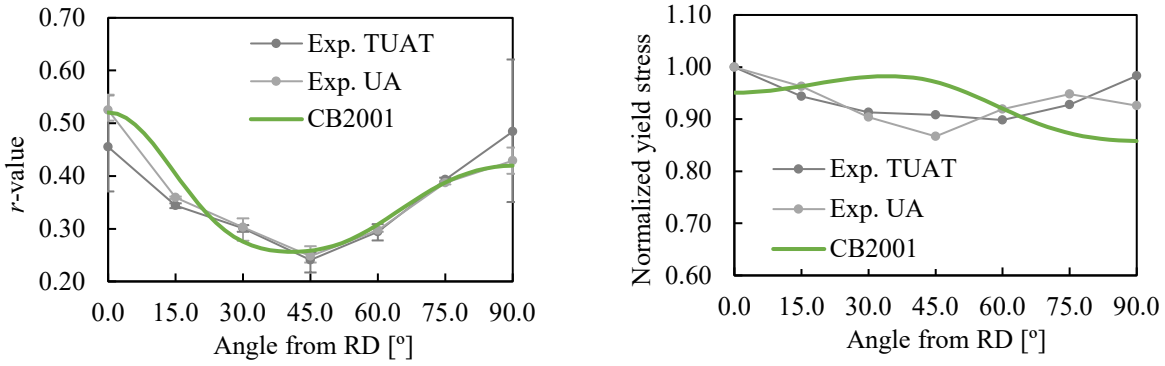

Fig. 2. Comparison between experimental and predicted: (a) r-values and (b) yield stresses.

Results and Discussion

The comparison between predicted and experimental punch force evolution is presented in Fig. 3, using both rigid and deformable tools in the numerical simulation. Besides, as previously mentioned, two different values of friction coefficient were used in the numerical analysis, namely μ=0.1 (Fig. 3 (a)) and μ=0.05 (Fig. 3 (b)). The drawing force is accurately described using μ=0.1 while the ironing force is clearly overestimated. Reducing the friction coefficient to μ=0.05 leads to a global reduction of the punch force during the drawing stage but, the ironing force is still overestimated. The increase of the punch force at approximately 35 mm of punch displacement results from the thickening of the blank during the drawing operation, leading to a thickness larger than the gap between the punch and the die (1.2 mm), i.e., results from the ironing. For both values of friction coefficient, the effect of the elastic deformation of the forming tools on the predicted drawing force is negligible. Nevertheless, the ironing force is reduced when the elastic deformation of the forming tools is considered in the numerical simulation. This is a consequence of the slight increase of the die opening diameter and, consequently, of the gap, due to the high values of contact pressure arising during the ironing stage of the cylindrical cup. Although the die in model #1 is stiffer than the one of model #2 (see Fig. 1), the bigger differences in the punch force only arise after 45 mm of punch displacement, i.e., when the cup wall is sliding over the vertical surface of the tools.

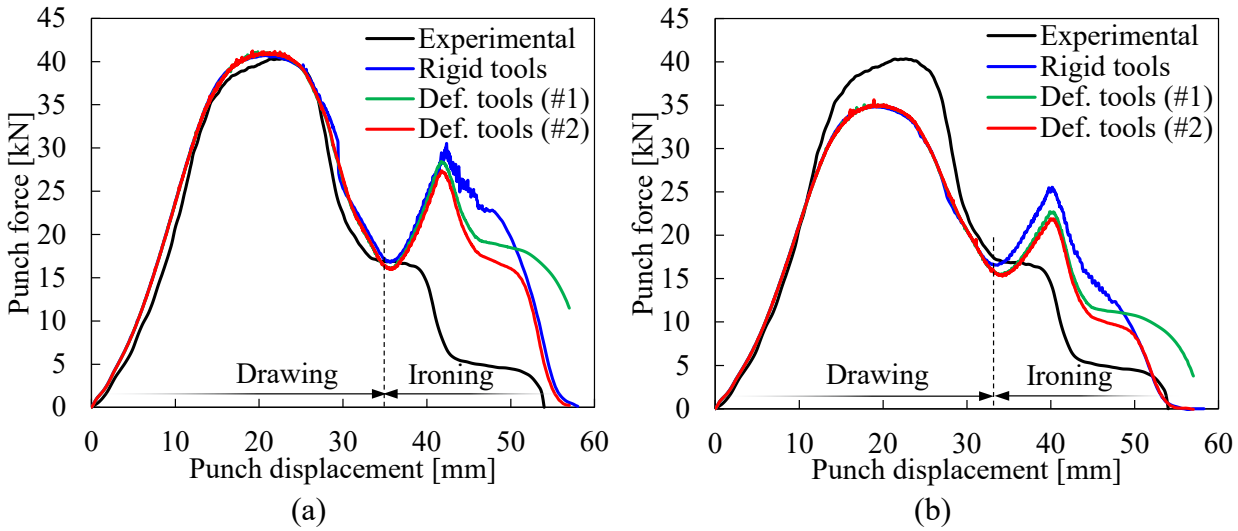

Fig. 3. Comparison between experimental [5] and numerical punch force evolution using different values of friction coefficient in the numerical analysis: (a) μ=0.1; (b) μ=0.05.

The numerical prediction of the blank-holder force evolution is presented in Fig. 4, for the different values of friction coefficient used in the numerical analysis. Regarding the rigid tools, the blank-holder force is kept constant (magnitude of 40±4 kN) by adjusting the position of the blank-holder. On the other hand, when the deformable tools are considered in the numerical model, the blank-holder force is proportional to the axial compression of the hollow cylinder. Thus, the blank-holder force increases slightly until about 25 mm of punch displacement (thickening of the flange) and then decreases quickly. At about 30 mm of punch displacement the stopper is activated, i.e., the gap between the blank-holder and the die decreases to 1.0 mm. The models with a lower friction coefficient predict the loss of contact between the blank and the blank-holder earlier (punch displacement lower than 30 mm) due to the reduction of the restraining forces. This effect is also visible in the punch force evolution, with a sudden drop, as shown in Fig. 3. This also means that

the models that use a lower value for friction coefficient predict lower strain values in the radial direction of the blank during this stage of the forming process.

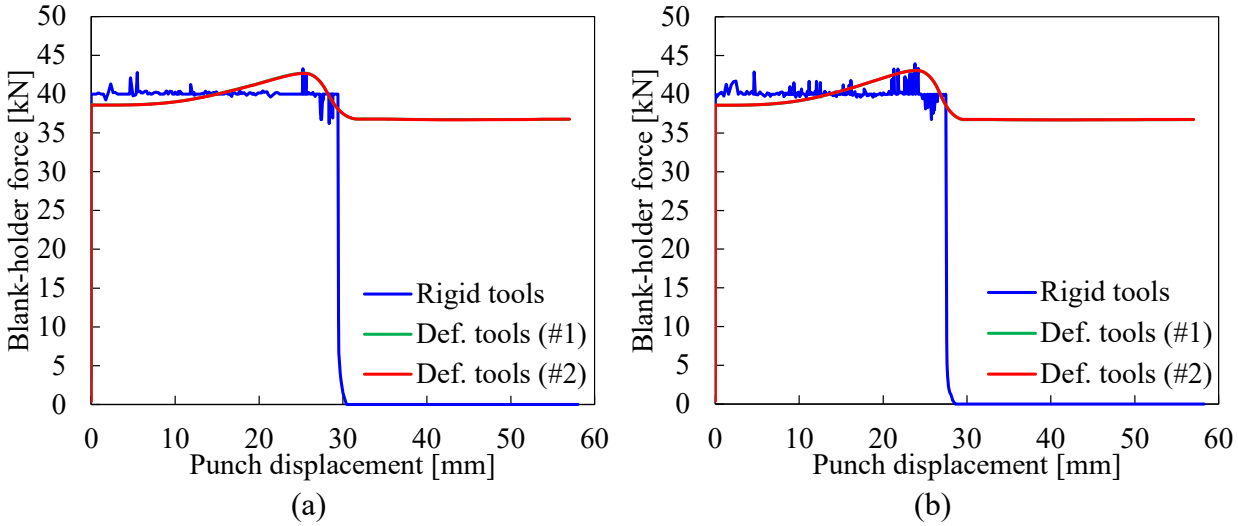

Fig. 4. Numerical prediction of the blank-holder force evolution using different values of friction coefficient in the numerical analysis: (a) μ=0.1; (b) μ=0.05.

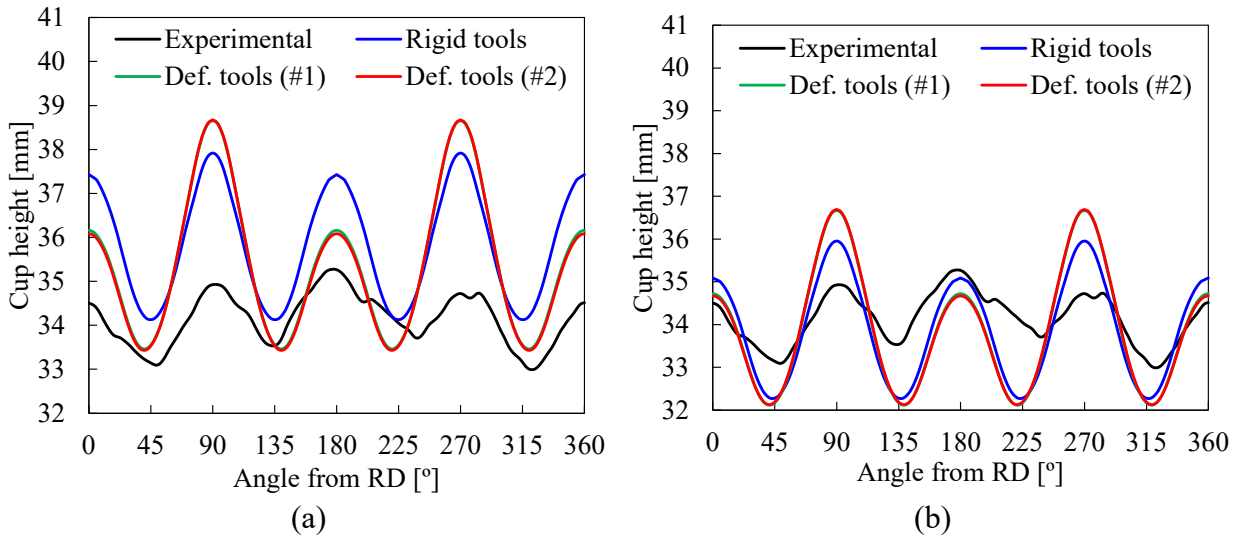

Fig. 5. Comparison between experimental [5] and numerical earing profile using different values of friction coefficient in the numerical analysis: (a) μ=0.1; (b) μ=0.05.

The comparison between the predicted and the experimental earing profile is presented in Fig. 5, using both rigid and deformable tools in the numerical simulation. The stiffness of the die has a negligible effect on this geometrical parameter. The decrease of the friction coefficient from μ=0.1 (Fig. 5 (a)) to μ=0.05 (Fig. 5 (a)) leads to a global decrease of the cup height. The amplitude of the ears experimentally measured is clearly overestimated by the numerical simulation, either using rigid or deformable tools. However, both the number of ears and the position of the valleys/peaks is accurately predicted. This can be related with the accurate description of the in-plane evolution of the *r*-values, while the overestimation of the amplitude of the ears can be associated with the less accurate prediction of the yield stress in-plane distribution, as shown in Fig. 1 and detailed in [5].

Whatever the friction coefficient adopted, the elastic deformation of the forming tools leads to the increase of the cup height in the transverse direction and a decrease in the rolling one. Nevertheless, the effect between the rolling direction and 45º is more evident for μ=0.1, corroborating the uneven distribution of the contact forces in the flange for anisotropic materials [11]. Considering the lower value of friction coefficient (μ=0.05), the elastic deformation of the forming tools leads to a slight increase (about 0.5 mm) of the amplitude of the ears. On the other hand, for μ=0.1 the amplitude of the ears increases about 1.7 mm in comparison with the results obtained using rigid tools. In both cases, the elastic deformation of the forming tools leads to a larger deviation from the experimental earing profile.

The distribution of the equivalent plastic strain is presented in Fig. 6, for the model that considers the deformation of the tools (#2), comparing the two different values of friction coefficient. The global increase of the cup height generated by the increase of the friction coefficient (see Fig. 5) results from a larger plastic strain at the cup bottom, as shown in Fig. 6. The ironing force when the cup wall is sliding between the punch and the die increases from 9.5 kN, when using μ=0.05, to 16.5 kN, for μ=0.1 (see Fig. 3). This increase of the punch force leads to a thinning of the cup bottom. Indeed, the predicted thickness in the middle of the cup bottom is reduced from 0.938 mm for μ=0.05 to 0.900 mm for μ=0.1.

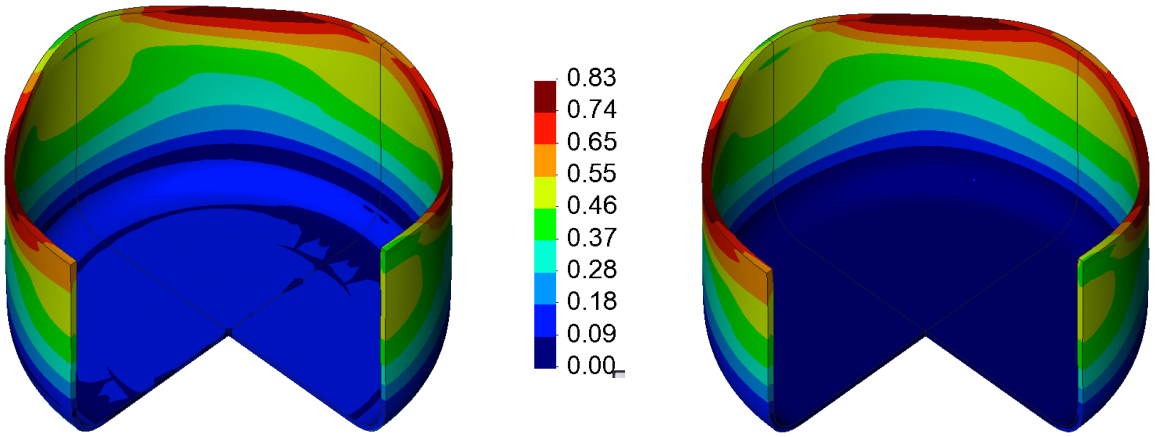

Fig. 6. Predicted equivalent plastic strain distribution considering the deformable tools (#2) described by solid elements using different values of friction coefficient: (a) μ=0.1; (b) μ=0.05.

Fig. 7 (a) compares the position of the outer radius of the blank along the circumferential direction, when using deformable tools (model #2) and the two values of friction coefficient, for two values of punch displacement. For a punch displacement of ~23 mm, there is still a flange (radius higher than 41.2 mm, which corresponds to the die opening radius plus the die shoulder radius). On the other hand, for a punch displacement of ~30 mm, the blank lost contact with the blank-holder (see Fig. 4). The results show a small effect of the friction coefficient on the draw-in, confirming that the increase of the friction coefficient constrains the radial movement of the flange. Fig. 7 (b) compares the thickness of the blank rim along the circumferential direction, for the same instants. The compression of the flange along the circumferential direction imposes an increase of the thickness. On the other hand, some locations present thinning (close to 90º) when the blank partially loses contact with the blank-holder, causing some pinching of the blank still in contact with the blank-holder (see Fig. 7 (a)). Globally, the lower value of the friction coefficient leads to slightly higher thickening, close to 45º. A higher thickness value should correspond to a higher contact pressure between the blank and the ironing tools (die and punch). Nevertheless, this seems to have a negligible impact in the ironing force evolution (see Fig. 3), because of the lower

friction coefficient. In fact, for both values of the friction coefficient in the simulations performed with deformable tools the ironing force presents an identical slope, between a punch displacement of ~ 36 mm and ~ 40 mm. Then, the force starts to drop in the numerical simulations performed with μ=0.05, while it keeps on increasing for μ=0.10, until a punch displacement of ~ 42 mm. This seems to be mainly dictated by the difference in the height of the cup, which is approximately 2 mm higher at the end of the forming, for the simulations performed with μ=0.10 (see Fig. 5). Note that, as previously mentioned, the increase of the friction coefficient constrains the radial movement of the flange, leading to a slightly lower draw-in (see Fig. 7 (a)) and a larger plastic strain at the cup bottom (see Fig. 6).

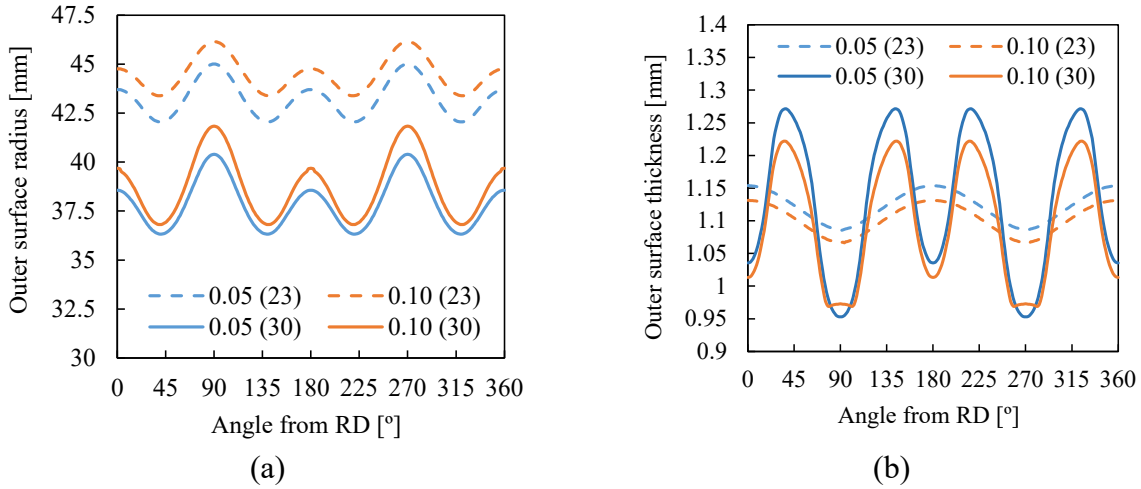

Fig. 7. Comparison between numerical distribution along the circumferential direction in the outer surface: (a) radius and (b) thickness, for a punch displacement of ~23 mm and 30 mm, using different values of friction coefficient (μ=0.1; μ=0.05) and deformable tools (model #2).

The comparison between predicted and experimental cup wall thickness distribution along the circumferential direction is presented in Fig. 8, which was evaluated at three different values of cup height (H), using both rigid and deformable tools in the numerical simulation. The decrease of the friction coefficient from μ=0.1 (Fig. 8 (a)) to μ=0.05 (Fig. 8 (b)) leads to a global increase of the final wall thickness, particularly at locations close to the cup bottom. In fact, using the largest value of friction coefficient (μ=0.1), the cup wall thickness is underestimated by the numerical models (rigid and deformable tools) at all locations, as shown in Fig. 8 (a). The largest difference between numerical and experimental data occurs for H=30 mm, where the numerical simulation considering rigid tools predicts a maximum value equal to the gap between the punch and the die. On the other hand, considering the elastic deformation of the forming tools, the final wall thickness is up to 0.03 mm larger than the nominal gap between the punch and the die. The comparison with the evolution presented in Fig. 7 (b) confirms that the ironing contributes to the uniformization of the thickness.

Due to the material anisotropy, the effect of the deformation of the tools is non-uniform along the circumferential direction. Thus, the thickness predicted using deformable tools is higher around the rolling direction and lower around the transverse direction (in comparison with the prediction obtained with rigid tools). The smaller difference between numerical and experimental thickness was obtained for the lower value of friction coefficient (μ=0.05), for which the predicted ironing force is closer to the experimental measurement (see Fig. 3). Nevertheless, the value is still higher than the experimental one, although the drawing force is clearly underestimated. This corroborates the difficulties in describing both process conditions using a constant value for the friction

coefficient. The results indicate that the friction coefficient between the blank and the die is very low during the ironing operation due to the high levels of contact pressure (see also [5]). The average thickness evaluated both at H=10 mm and H=20 mm is accurately predicted using the lower friction coefficient (see Fig. 8 (b)), although there is a larger variation of the cup wall thickness predicted by the numerical models along the circumferential direction (anisotropic behaviour). This variation is influenced by the yield criterion adopted, as discussed in [5].

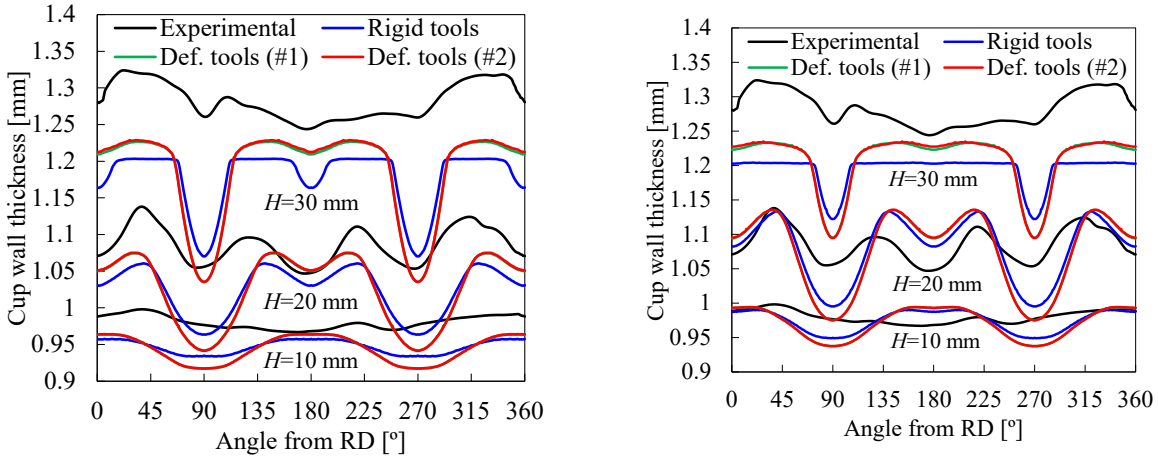

Fig. 8. Comparison between experimental [5] and numerical cup wall thickness distribution along the circumferential direction evaluated at three different cup height values using different values of friction coefficient in the numerical analysis: (a) μ=0.1; (b) μ=0.05.

Summary

The Swift cup drawing test proposed at the benchmark EXACT was used to study the importance of the stiffness of the forming tools on the numerical predictions. Accordingly, the numerical results are compared with the experimental ones. When considering a small value for the friction coefficient, the punch force is underestimated in the drawing stage and overestimated in the ironing stage. Besides, the decrease of the friction coefficient leads to a global decrease of the cup height. The smaller difference between numerical and experimental thickness was obtained for the lower value of friction coefficient. Considering the deformation of the forming tools in the numerical simulation, the main conclusions are:

- The predicted ironing force is significantly reduced, while the effect on the predicted drawing force is negligible;
- The amplitude of the ears is enlarged, particularly for the largest value of friction coefficient;
- The predicted wall thickness is larger than the gap between the punch and the die.

Acknowledgments

The authors gratefully acknowledge the financial support of the Portuguese Foundation for Science and Technology (FCT) under projects with reference 2022.08459.PTDC, UIDB/00285/2020 and LA/P/0112/2020.

References

[1] M. Burkart, P. Essig, M. Liewald, M. Beck, M. Mueller, Compensation of elastic die and press deformations during sheet metal forming by optimizing blank holder design, in: IOP Conf Ser Mater Sci Eng, IOP Publishing Ltd, 2020. https://doi.org/10.1088/1757-899X/967/1/012074.

[2] R. Lingbeek, Virtual tool reworking new strategies in die design using finite element forming simulations, PhD Thesis, University of Twente (2008).

[3] J. Pilthammar, M. Sigvant, S. Kao-Walter, Introduction of elastic die deformations in sheet metal forming simulations, Int. J. Solids Struct. 151 (2018) 76-90. https://doi.org/10.1016/j.ijsolstr.2017.05.009

[4] F. Abbasi, A. Sarasua, J. Trinidad, N. Otegi, E. Saenz de Argandoña, L. Galdos, Substitutive press-bolster and press-ram models for the virtual estimation of stamping-tool cambering, Materials. 15 (2022). https://doi.org/10.3390/ma15010279

[5] A.M. Habraken, T.A. Aksen, J.L. Alves, R.L. Amaral, E. Betaieb, N. Chandola, L. Corallo, D.J. Cruz, L. Duchêne, B. Engel, E. Esener, M. Firat, P. Frohn-Sörensen, J. Galán-López, H. Ghiabakloo, L.A.I. Kestens, J. Lian, R. Lingam, W. Liu, J. Ma, L.F. Menezes, T. Nguyen-Minh, S.S. Miranda, D.M. Neto, A.F.G. Pereira, P.A. Prates, J. Reuter, B. Revil-Baudard, C. Rojas-Ulloa, B. Sener, F. Shen, A. van Bael, P. Verleysen, F. Barlat, O. Cazacu, T. Kuwabara, A. Lopes, M.C. Oliveira, A.D. Santos, G. Vincze, Analysis of ESAFORM 2021 cup drawing benchmark of an Al alloy, critical factors for accuracy and efficiency of FE simulations, Int. J. Mater. Forming 15 (2022) 1-96. https://doi.org/10.1007/s12289-022-01672-w

[6] D.M. Neto, J. Coër, M.C. Oliveira, J.L. Alves, P.Y. Manach, L.F. Menezes, Numerical analysis on the elastic deformation of the tools in sheet metal forming processes, Int. J. Solids Struct. 100 (2016) 270-285. https://doi.org/10.1016/j.ijsolstr.2016.08.023

[7] L.F. Menezes, C. Teodosiu, Three-dimensional numerical simulation of the deep-drawing process using solid finite elements, J. Mater. Process. Technol. 97 (2000) 100-106. https://doi.org/10.1016/S0924-0136(99)00345-3

[8] J. Coër, H. Laurent, M.C. Oliveira, P.Y. Manach, L.F. Menezes, Detailed experimental and numerical analysis of a cylindrical cup deep drawing: Pros and cons of using solid-shell elements, Int. J. Mater. Forming 11 (2018) 357-373. https://doi.org/10.1007/S12289-017-1357-4/FIGURES/21

[9] D.M. Neto, M.C. Oliveira, L.F. Menezes, J.L. Alves, Applying Nagata patches to smooth discretized surfaces used in 3D frictional contact problems, Comput. Methods Appl. Mech. Eng. 271 (2014). https://doi.org/10.1016/j.cma.2013.12.008

[10] O. Cazacu, F. Barlat, Generalization of Drucker's yield criterion to orthotropy, Math. Mech. Solids 6 (2001) 613-630. https://doi.org/10.1177/108128650100600603

[11] D.M. Neto, M.C. Oliveira, R.E. Dick, J.L. Alves, L.F. Menezes, Non-Uniform Effect of the Contact Conditions on the Earing Profile in Cylindrical Cups of Anisotropic Materials, Key Eng. Mater. 926 (2022) 1188-1194. https://doi.org/10.4028/p-9i8j3o